

Direct Evidence for Tetrahedral Interstitial Er in Si

U. Wahl, A. Vantomme, J. De Wachter, R. Moons, and G. Langouche

Instituut voor Kern- en Stralingsfysica, University of Leuven, Celestijnenlaan 200 D, B-3001 Leuven, Belgium

J. G. Marques

CFNUL, Avenida Professor Gama Pinto 2, P-1699 Lisboa Codex, Portugal

J. G. Correia, and ISOLDE collaboration
CERN-PPE, CH-1211 Geneva 23, Switzerland

(Received 1 May 1997)

We report on the lattice location of Er in Si using the emission channeling technique. The angular distribution of conversion electrons emitted by the decay chain ^{167}Tm ($t_{1/2}=9.25$ d) \rightarrow $^{167\text{m}}\text{Er}$ (2.28 s) was monitored with a position sensitive detector following room temperature implantation and annealing up to 950°C. Our experiments give direct evidence that Er is stable on tetrahedral interstitial sites in FZ Si. We also confirm that rare earth atoms strongly interact with oxygen, which finally leads to their incorporation on low-symmetry lattice sites in CZ Si.

PACS numbers: 61.72 Tt, 61.72 Yx

Rare earth doping of Si is known to result in the formation of luminescent centers and is considered as a possible way to manufacture Si-based optoelectronic devices [1]. Among the various rare earth elements, Er is of special interest since its atomic transition at 1.54 μm matches the absorption minimum of SiO_2 , a highly desirable feature both for signal transmission through glass fiber cables and optical on-chip communication. Luminescence at this wavelength from Er-implanted Si was already established several years ago [2]. Meanwhile Er-based light-emitting diodes (LEDs) operating at room temperature have been reported [3]. The basic understanding of Er luminescence in Si, however, is far from complete. This concerns both the lattice sites of Er and the role of co-dopants such as O, N or F, which were found to have a beneficial influence on luminescence yield. Photoluminescence (PL) spectroscopy studies have identified a number of Er-related centers with different crystal surroundings in Si [4]. The most intense PL yield was due to two centers having cubic and axial symmetry, respectively. While the cubic center occurred in both float-zone (FZ) and Czochralski (CZ) Si and was attributed to tetrahedral (T) interstitial Er, the center with axial symmetry was only observed in CZ Si and ascribed to Er-O complexes. The existence of tetrahedral interstitial Er would be also in agreement with theoretical studies, which predict that T sites are the most stable sites for all oxidation states of isolated Er atoms in Si [5]. Direct lattice location using the Rutherford backscattering (RBS) channeling technique only suggested substitutional [6] or hexagonal (H) interstitial Er [7,8]. The reasons for these discrepancies, however, are unclear.

To study the lattice sites and damage recovery after rare earth implantation, we have applied conversion electron emission channeling [9] combined with position sensitive

detection. Emission channeling makes use of the fact that charged particles emitted from radioactive isotopes in single crystals experience channeling or blocking effects along low-index crystal directions. This leads to an anisotropic particle emission yield from the crystal surface which depends in a characteristic way on the lattice sites occupied by the emitter atoms. While this technique as such is not new and, in case of rare earths, was already used once for the lattice location of ^{175}Yb in Si [10], we have for the first time applied position-sensitive detection of electrons. This new approach further increases the experimental efficiency by one to two orders of magnitude and allows a much faster, easier and more precise determination of lattice sites.

We used the radioactive isotope ^{167}Tm ($t_{1/2}=9.25$ d) which decays into two excited states of ^{167}Er with half lives of 1.5 ns and 2.28 s, respectively (Fig. 1). While the 1.5 ns state emits L and M conversion electrons of 48 and 56 keV energy, the decay of the 2.28 s state $^{167\text{m}}\text{Er}$ is accompanied by K, L and M electrons of 150, 199 and 206 keV. Both types of electrons can be used for lattice location purposes, and they probe the lattice sites of ^{167}Er during different time windows following the decay of ^{167}Tm . 60 keV implantations of ^{167}Tm into Si single crystals were done at the ISOLDE facility [11] at CERN using a 1 mm beam spot. Four different samples were investigated, *p*-Si:B FZ (10 k Ωcm , $\langle 111 \rangle$ orientation, implanted dose 4.8×10^{13} cm^{-2}), *n*-Si:P FZ (>4 k Ωcm , $\langle 111 \rangle$, 5.1×10^{13} cm^{-2}), *p*-Si:B CZ (5-14 Ωcm , $\langle 100 \rangle$, 4.4×10^{13} cm^{-2}) and *n*-Si:P CZ (1-10 Ωcm , $\langle 100 \rangle$, 3.5×10^{13} cm^{-2}). Following room temperature implantation, annealing was done under vacuum better than 10^{-5} mbar. In order to measure the conversion electron emission yield as a function of angle towards different crystallographic directions we used a



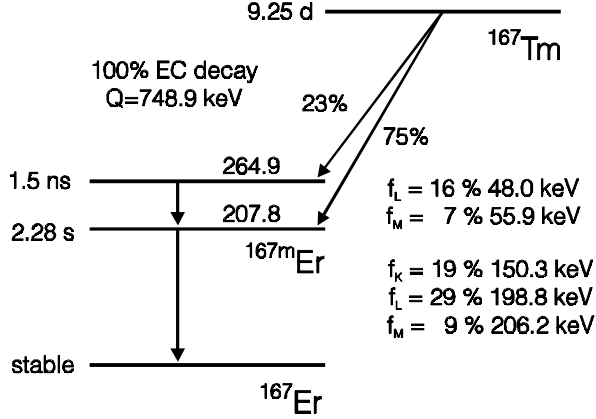


FIG. 1: Simplified decay scheme of $^{167}\text{Tm}/^{167\text{m}}\text{Er}$ (some low-intensity EC transitions are not shown). f_K , f_L , and f_M are conversion electron intensities with reference to the decay of ^{167}Tm .

$30 \times 30 \text{ mm}^2$ Si detector (0.5 mm thick, 5 keV FWHM energy resolution), consisting of 22×22 "pads" (or pixels) of $1.3 \times 1.3 \text{ mm}^2$ size, which was mounted at a distance of 285 mm from the sample. Such detector systems were recently developed at CERN in the context of high-energy physics collider experiments [12], and we have adapted them for use in electron emission channeling.

Figures 2 (a), (b) and (c) show the normalized emission yield of conversion electrons from the 2.28 s state $^{167\text{m}}\text{Er}$ in the *p*-Si FZ crystal at the end of an isochronal annealing sequence from room temperature up to 900°C [10 min, steps of 100 K, cf. Fig. 3 (a)]. Clearly visible are prominent channeling effects along axial $\langle 100 \rangle$ and $\langle 111 \rangle$ and planar $\{110\}$ directions, and less pronounced channeling effects along $\{100\}$ and $\{211\}$. On the contrary, the axial $\langle 110 \rangle$ and planar $\{111\}$ and $\{311\}$ directions all show yields close to unity or below. The combination of these patterns is direct evidence that the majority of $^{167\text{m}}\text{Er}$ occupies sites close to the tetrahedral interstitial (T) position. While T sites are perfectly aligned with $\langle 100 \rangle$, $\langle 111 \rangle$, $\{100\}$, $\{110\}$ and $\{211\}$ lattice directions, leading to channeling of electrons emitted from these sites, they are interstitial with respect to $\langle 110 \rangle$ atomic axes and $\{111\}$ and $\{311\}$ atomic planes, causing yield minima along these directions [13]. Note that due to the negative charge of the conversion electrons this is essentially the opposite behaviour to that observed for alpha emitter atoms on tetrahedral sites [14]. Significant contributions from emitters on substitutional (S) sites can be ruled out, since these would show up as channeling effects along $\langle 110 \rangle$, $\{111\}$ and $\{311\}$ directions. A comparable argument holds for ruling out hexagonal (H) sites, which are located clearly off all $\langle 100 \rangle$ atomic axes and $\{100\}$ atomic planes and are incompatible with the observed channeling along $\langle 100 \rangle$ and $\{100\}$.

In order to characterize the Er lattice location more precisely, we have carried out computer simulations of emission yields for a variety of sites. The concept of electron emission channeling simulations is based on the

dynamical theory of electron diffraction and described in detail in Refs. [9,13]. Due to quantum-mechanical diffraction patterns, the angular dependence of the electron emission yield shows a rich fine structure, which requires us to take into account a fine mesh of small angular steps. We therefore considered a range of $\pm 3^\circ$ around the $\langle 100 \rangle$, $\langle 110 \rangle$ and $\langle 111 \rangle$ directions in steps of $\Delta\chi = \Delta\gamma = 0.05^\circ$, resulting in characteristic two-dimensional patterns of electron emission probability for each lattice site. Quantitative information is then obtained comparing the fit of simulated patterns to the observed yields. The fit procedures used for this purpose are modified versions of those given in Ref. [15] for the case of alpha emission channeling patterns. The size and shape of the detector pads were taken into account during fitting by averaging over the simulated yield falling within the angular range ($0.26^\circ \times 0.26^\circ$) of one pad. We considered S, T, H, bond center (BC), anti bonding (AB), split $\langle 100 \rangle$ (SP) and the so-called Y and C sites (cf. Ref. [14]), as well as $\langle 111 \rangle$ and $\langle 100 \rangle$ displacements between these sites and mixtures of several sites. Figures 2 (d), (e) and (f) show the best fit results, which were, consistently for all three axes, obtained for a displacement of $d = 0.43(8) \text{ \AA}$ from the T site. The mean value for the fraction of emitter atoms on these sites derived from the fits in Fig. 2 is 93(7)%. Ideal T sites did not satisfactorily describe the experimental patterns, leading to a 30% increase in the chi square of fit. Note, however, that for such small displacements the channeling effect can only give information on the projected mean displacement of the emitter atoms. This means that it is neither possible to determine the direction of displacement, e.g., whether from T to H, T to AB or T to Y sites, nor whether there exists only one specific or an ensemble of *d* values in the range 0-0.6 \AA with a mean value of $d \approx 0.43 \text{ \AA}$. We consider it very likely that we have such a mixture of displacements, with, e.g., the majority of Er on ideal T sites and some smaller part (10-15%) close to nearby Y sites. We also fitted the emission channeling effects of the 48 keV and 56 keV electrons originating from the 1.5 ns state in ^{167}Er and obtained the same site preference as discussed above, i.e. near-T with $d = 0.44(10) \text{ \AA}$, with similar fractions (cf. Fig. 3). This directly shows that the majority of ^{167}Er already occupies the near-T sites within less than 1 ns after the ^{167}Tm decay.

Figure 3 displays the Er fractions on near-T sites observed during isochronal annealing sequences for all four Si crystals. Despite the fact that the $^{167}\text{Tm}/^{167}\text{Er}$ probes are located in a highly defective surrounding, electron emission channeling effects were already clearly visible directly following room temperature implantation. The observed channeling patterns could be fitted well by an equivalent of 20-25% near-T emitter atoms in a perfect lattice and the remainder on so-called "random sites". Random sites are lattice positions associated with negligible anisotropy in emission yield, i.e. sites of very low crystal symmetry, or sites in heavily damaged or amorphous surroundings. Upon annealing to 600°C the electron emission channeling effects increased markedly.

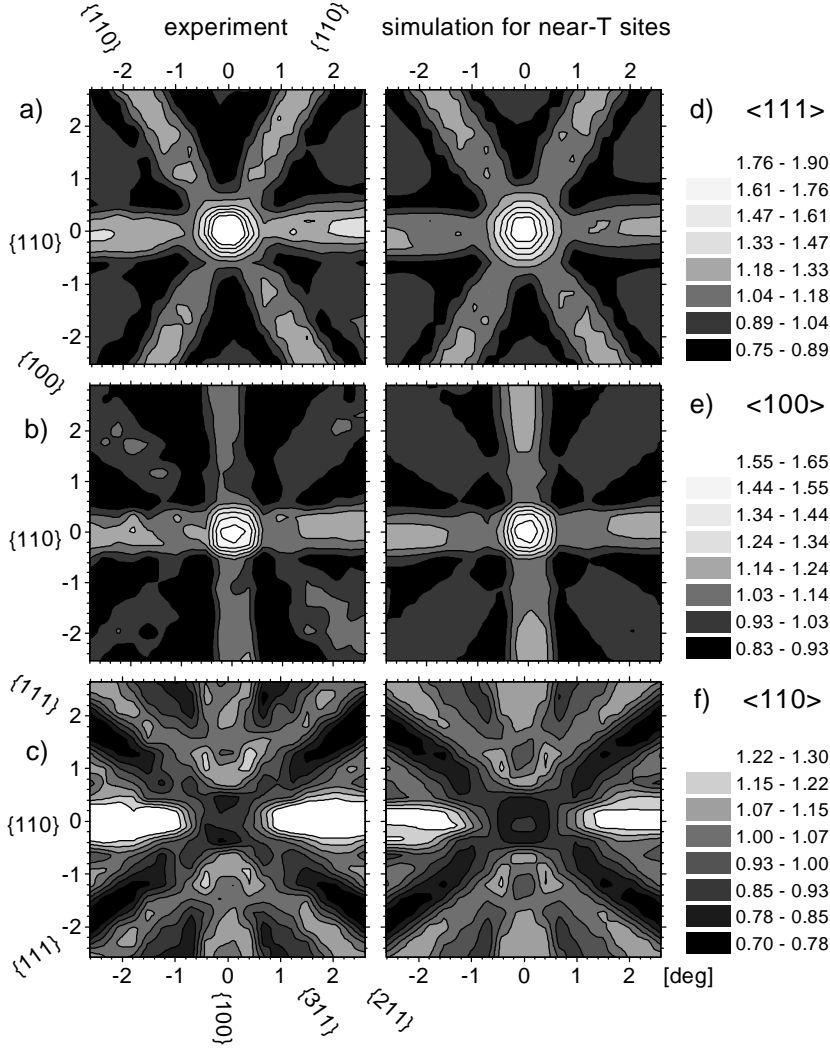


FIG. 2: a, b, c: channeling patterns from $^{167\text{m}}\text{Er}$ (2.28 s) following room temperature implantation of ^{167}Tm into *p*-Si FZ and after finishing the annealing sequence to 900°C. Shown are normalized electron emission yields from the combined intensity of 150, 198 and 206 keV electrons in the vicinity of $\langle 111 \rangle$, $\langle 100 \rangle$ and $\langle 110 \rangle$ directions. d,e,f: best fits of simulated patterns to the experimental yields, corresponding to 86%, 95% and 99% of emitter atoms on sites which are displaced by 0.43 Å from the T site.

We attribute this to the well-known solid phase epitaxial regrowth of implanted Si in the temperature range 550-600°C [16]. As a result, the quality of the crystal lattice is restored to a large extent, and our measurements show that subsequently more than 90% of ^{167}Er emitter atoms are located on near-T sites. For annealing at 800°C and above, pronounced differences between FZ Si and CZ Si were observed. In FZ Si [Fig. 3 (a)], which typically has a small oxygen concentration of 10^{15} - 10^{16} cm $^{-3}$, a 10 min anneal at 900°C even further increased the near-T fraction by some percent. In the oxygen-rich CZ material (typically $[\text{O}] \approx 10^{17}$ - 10^{18} cm $^{-3}$), however, the fraction on near-T sites dropped markedly in both *p*- and *n*-Si [Fig. 3 (b)]. The channeling patterns obtained following 950°C annealing of CZ Si could be well fitted by assuming 25-35% of Er on near-T sites and the remainder on random

sites. In this case, within the statistical limits of our present data, we can not exclude that there is also a small fraction of distinct lattice sites of low symmetry involved, however, more than 10% on H sites can be ruled out.

In order to interpret our experimental results, let us first discuss to what extent the observed lattice sites of ^{167}Er might be influenced by the properties of the parent ^{167}Tm and its electron capture (EC) decay (Tm also seems to prefer interstitial sites in Si [10]). The ^{167}Er nucleus receives a recoil energy of 0.7 to 0.9 eV due to neutrino emission, and the initial electronic configuration contains a hole in the K shell. Both thermalization of nuclear recoil and electronic deexcitation via X-ray emission could in principle result in metastable configurations or relaxation to a stable lattice site. In order to directly monitor the thermal stability of tetrahedral Er in FZ Si, we have therefore also undertaken channeling measurements at 600°C and 900°C, with the same results as in the case of 20°C [cf. Fig. 3 (a)]. Since the diffusivity of Er in Si is $D \approx 10^{-15}$ cm 2 s $^{-1}$ at 900°C [3], its mean diffusion length $(6Dt)^{1/2}$ during the 3.27 s life time of the $^{167\text{m}}\text{Er}$ state is already around 14 Å, which should also allow Er to relax to its own most-stable lattice site. The near-T fraction measured after 2 h annealing of *n*-Si FZ at 900°C and subsequent cooling to room temperature is already significantly smaller [Fig. 3 (a)], but still much higher than in CZ Si for the 10 min anneals.

Assuming that the diffusivity of the parent Tm at 900°C is similar to Er, one estimates mean diffusion lengths of 190 Å within 10 min and 660 Å within 2 h. These values are comparable to the average distance between oxygen atoms, (around 130 Å in CZ Si and 600 Å in FZ Si) and somewhat larger than the mean distance to neighbouring Er or Tm (37 Å in the peak of the implantation profile where the Tm/Er concentration reaches a maximum of 2×10^{19} cm $^{-3}$). The diffusivity of oxygen ($D = 0.13$ cm 2 s $^{-1}$ exp[-2.53 eV/kT]) [17], however, is much larger than the one of Er, and can not be neglected. A scenario which is compatible with our observations in CZ Si is as follows. Some Er atoms capture oxygen already far below 900°C, but still reside on near-T sites, and these centers finally act as precipitation nuclei for the remaining rare earths. Ref.

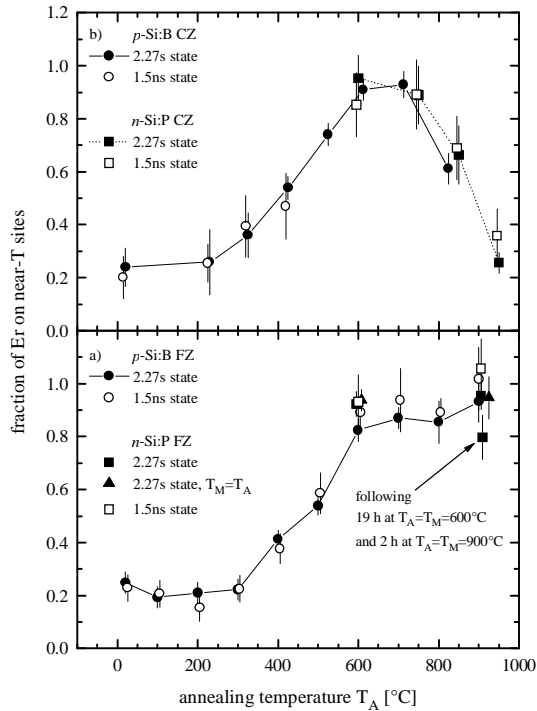


FIG. 3. Isochronal annealing sequences (10 min, measurements at $T_M=20^\circ\text{C}$, unless indicated otherwise) for the fraction of ^{167}Er on near-T sites. Panel (a) shows data from FZ Si, panel (b) from CZ Si. Note that for both types of Si it is also discriminated between n- and p-Si and results obtained from the different conversion electrons emitted by the two excited nuclear states of ^{167}Er . After completing the annealing sequence of the n-Si FZ at 900°C , the measuring temperature was raised to 600°C for 19 h, and 900°C for 2 h, and then lowered back to room temperature.

[4], however, states that maximizing the PL intensity from Er-O complexes required annealing at 900°C . This could indicate that oxygen diffusion is inhibited by pairing with implantation-induced defects, so that the massive formation of Er-O complexes requires the onset of Er mobility around 900°C .

In summary, we have clearly demonstrated that Er is stable on near-tetrahedral interstitial sites in FZ Si up to typical annealing temperatures used in the processing of implanted wafers. Our results are in accordance with theoretical predictions for isolated Er in Si [5] and also with the existence of cubic Er centers observed by PL [4], but put the interpretation of previous RBS studies of Si:Er [6-8] into question. In oxygen rich CZ Si we observed a distinct decrease in the near-tetrahedral Er fraction for annealing at 800°C and above, indicating a strong interaction of the parent Tm with O-related defects. On the other hand, since the concentration of implanted Tm/Er is identical in FZ and CZ Si, it seems that the formation of simple clusters of Tm/Er is less efficient. In order to clarify

the role of oxygen, further experiments are planned, applying both higher and lower ^{167}Tm implantation doses (a further reduction of a factor 10 is feasible), and also O co-implantation. Since the conversion electron transitions result in stable ^{167}Er in its ground state, this probe atom also offers the opportunity to first investigate the Er lattice sites by emission channeling followed by a characterization of the luminescence properties of the same samples.

We would like to thank P. Weilhammer, A. Czermak, S.G. Jahn, P. Jalocha, A. Rudge and F. Schopper for providing the position-sensitive detectors, and H. Hofsäss for the permission to use his electron channeling simulation code "Manybeam". J.G.M. and J.G.C. acknowledge JNICT (Portugal) for grants under the Praxis XXI program, A.V. the post-doctoral research program of the Fund for Scientific Research, Flanders (FWO).

- [1] S. S. Iyer and Y. H. Xie, *Science* 260, 40 (1993).
- [2] H. Ennen, J. Schneider, G. Pomrenke, and A. Axmann, *Appl. Phys. Lett.* 43, 943 (1983).
- [3] F. Y. G. Ren et al, *Mat. Res. Soc. Symp. Proc.* 301, 87 (1993).
- [4] H. Przybylinska et al, *Phys. Rev. B* 54, 2532 (1996).
- [5] M. Needels, M. Schlüter, and M. Lannoo, *Phys. Rev. B* 47, 15533 (1993).
- [6] Y. S. Tang, Z. Jingping, K. C. Heasman, and B. J. Sealy, *Sol. State Comm.* 72, 991 (1989).
- [7] A. Kozanecki, R. Wilson, B. J. Sealy, J. Kaczanowski, and L. Nowicki, *Appl. Phys. Lett.* 67, 1847 (1995).
- [8] A. Kozanecki, J. Kaczanowski, R. Wilson, and B. J. Sealy, *Nucl. Instr. Meth. B* 118, 709 (1996).
- [9] H. Hofsäss and G. Lindner, *Phys. Rep.* 201, 123 (1991).
- [10] E. Uggerhøj and J. U. Andersen, *Can. J. Phys.* 46, 543 (1968).
- [11] E. Kugler et al, *Nucl. Instr. Meth. B* 70, 41 (1992).
- [12] P. Weilhammer, E. Nygård, W. Dulinski, A. Czermak, F. Djama, S. Gadomski, S. Roe, A. Rudge, F. Schopper and J. Strobel, *Nucl. Instr. Meth. A* 383, 89 (1996).
- [13] H. Hofsäss, *Hyperfine Interactions* 97, 247 (1996).
- [14] U. Wahl, *Phys. Rep.* 280, 145 (1997).
- [15] U. Wahl, S.G. Jahn, M. Restle, C. Ronning, H. Quintel, K. Bharuth-Ram, H. Hofsäss, and the ISOLDE collaboration, *Nucl. Instr. Meth. B* 118, 76 (1996).
- [16] E. Rimini, *Ion Implantation: Basics to Device Fabrication* (Kluwer, Boston, 1995) p 173 ff.
- [17] *Landolt-Börnstein, Numerical Data and Functional Relationships in Science and Technology*, Vol. 22b, edited by M. Schulz (Springer, Berlin, 1989).